Korean J. Math. **23** (2015), No. 1, pp. 171–180
http://dx.doi.org/10.11568/kjm.2015.23.1.171

POINTWISE BEHAVIOR OF THE POTENTIAL IN ANOMALOUS LOCALIZED RESONANCE: A NUMERICAL STUDY

Junyong Eom

Abstract. It is discovered in [7] that a dielectric material is coated by a plasmonic material of negative permittivity with dissipation, then cloaking by anomalous localized resonance may occur as the dissipation tends to zero. In this paper, we investigate numerically the pointwise behavior of the potential in the shell when cloaking by anomalous localized resonance (CALR) occurs. By changing locations a dipole source, we can observe some localizing properties of the potential in the shell.

1. Introduction

Let Ω be a bounded domain in $\mathbb{R}^2$ and D be a domain compactly contained in Ω. Let $\delta > 0$ be a loss parameter and

$$\varepsilon_\delta = \begin{cases} 1 & \text{in } \mathbb{R}^2 \setminus \overline{\Omega}, \\ -1 + i\delta & \text{in } \overline{\Omega} \setminus \overline{D}, \\ 1 & \text{in } D. \end{cases} \tag{1}$$

For a given function f compactly supported in $\mathbb{R}^2 \setminus \overline{\Omega}$, satisfying

$$\int_{\mathbb{R}^2} f dx = 0,$$

Received December 26, 2015. Revised March 11, 2015. Accepted March 11, 2015.
2010 Mathematics Subject Classification: 35Q60.
Key words and phrases: cloaking, anomalous localized resonance, plasmonic structure.

we consider the following problem :

$$\begin{cases} \nabla \cdot \varepsilon_\delta \nabla V_\delta = f & \text{in} \quad \mathbb{R}^2, \\ V_\delta(x) \to 0 & \text{as} \quad |x| \to \infty. \end{cases} \tag{2}$$

We emphasize that if $\delta > 0$ then the problem is elliptic and admits a unique solution. However, as δ tends to 0, the ellipticity breaks down and the solution V_δ exhibits a singular behavior. In fact, it is proved in [1] that if Ω and D are concentric disks, then

$$\limsup_{\delta \to 0} E_\delta = \infty \tag{3}$$

where

$$E_\delta = \int_{\Omega \setminus \overline{D}} \delta |\nabla V_\delta|^2 dx.$$

Moreover, it is shown in the same paper that if the Fourier coefficients of the Newtonian potential of f satisfies a certain gap condition, then

$$\lim_{\delta \to 0} E_\delta = \infty. \tag{4}$$

For instance, if the source function f is a polarizable dipole, i.e, $f(x) = a \cdot \nabla \delta_y(x)$ for a vector a and $y \in \mathbb{R}^2 \setminus \overline{\Omega}$ where δ_y is the Dirac mass at y, then the gap condition is satisfied and (4) holds, which was originally proved in [5]. Observe that (3) and (4) describe the behavior of solution in L^2-sense. In this paper, our interest lies in the pointwise behavior of the solution.

The problem (2) arises from the study of cloaking by anomalous localized resonance (CALR). The coefficient ε_δ in (1) represents the permittivity distribution of the structre. In particular, $-1 + i\delta$ in the shell $(\Omega \setminus D)$ indicates a plasmonic material of negative dielectric constant (with a dissipation δ). It is first shown in [5] that the dipole source f outside the structure can be cloaked by (4). This result was extended to general source f in [1]. There a general scheme based on the spectral theory of the Neumann-poincaré operator was developed to investigate CALR. In [7], a variational approach has been adapted to study on CALR. The structure considered in above mentioned work is the concentric disk. On the other hand, in [6], CALR for conforcal ellipses are characterized. In [2], it is shown that CALR does not occur when D and Ω are concentric balls in $\mathbb{R}^3$. On the other hand, it is proved in [4] that it is possible to make CALR occur in three dimensional spherical structure by using a shell with a special designed anisotropic dielectric constant. CALR is also connected to superlenses for which we refer to [8,9]

As shown in the next section, the solution to (2) is given in terms of Fourier series. It is a difficult task to investigate the pointwise behavior of a function given in terms of Fourier series. So, in this paper we study the pointwise behavior of V_δ numerically using matlab as a first step toward the difficult problem of pointwise behavior of the solution. The finding of this paper will serve as a basis for rigorous study in future.

2. The potential expressed by Fourier series

Let G be the fundamental solution to the Laplacian in $\mathbb{R}^2$ which is given by

$$G(x) = \frac{1}{2\pi}\ln|x|,$$

and let F be the Newtonian potential of f, that is

$$F(x) = \int_{\mathbb{R}^2} G(x-y)f(y)dy, \quad x \in \mathbb{R}^2.$$

Let Ω and D be disks centered at the origin of radii r_e and r_i, $(r_e > r_i)$ repectively, so that D is the core and $\Omega \setminus D$ is the shell. Then it is proved in [3] that the solution $V_\delta(r,\theta)$ in the shell is given by

$$V_\delta(r,\theta) = r_e \sum_{n\neq 0} \left[(2z_\delta+1)\frac{r_i^{2|n|}}{r^{|n|}} - (4z_\delta^2+2z_\delta)r^{|n|}\right] \frac{g_e^n e^{in\theta}}{|n|r_e^{|n|}(4z_\delta^2-\rho^{2|n|})}, \tag{5}$$

where $z_\delta = \frac{i\delta}{2(2-i\delta)}$, $\rho = \frac{r_i}{r_e}$, and

$$-\frac{\partial F}{\partial r}\bigg|_{r=r_e} = \sum_{n\neq 0} g_e^n e^{in\theta}. \tag{6}$$

Also the solution in the core and the matrix are given by

$$V_\delta(x) = \sum_{n\neq 0} \left[(4z_\delta^2-1)r^{|n|}\right] \frac{g_e^n e^{in\theta}}{|n|r_e^{|n|}(4z_\delta^2-\rho^{2|n|})},$$

and

$$V_\delta(x) = F(x) + r_e \sum_{n\neq 0} \left[2(r_i^{2|n|} - r_e^{2|n|}) \frac{z_\delta}{r^{|n|}} \right] \frac{g_e^n e^{in\theta}}{|n| r_e^{|n|} (4z_\delta^2 - \rho^{2|n|})}.$$

Suppose that f is a polarizable dipole, namely, $f(x) = a \cdot \nabla \delta_y(x)$ for a vector $a = (a_1, a_2) \in \mathbb{R}^2$ and $y \in \mathbb{R}^2 \setminus \overline{\Omega}$. Then $F(x) = a \cdot \nabla_x G(x-y)$. The fundamental solution G admits the expansion

$$G(x-y) = -\sum_{n=1}^{\infty} \frac{1}{2\pi n} \left[\frac{\cos n\theta_y}{r_y^n} r^n \cos n\theta + \frac{\sin n\theta_y}{r_y^n} r^n \sin n\theta \right],$$

where r_y, θ_y denote the radius and angle of y, respectively. So, we have

$$\begin{aligned} F(x) &= a \cdot \nabla_x G(x-y) \\ &= a_1 \sum_{n=1}^{\infty} \frac{-1}{2\pi} \left[\frac{\cos n\theta_y}{r_y^n} r^{n-1} \cos n\theta + \frac{\sin n\theta_y}{r_y^n} r^{n-1} \sin n\theta \right] \cos\theta \\ &\quad + a_1 \sum_{n=1}^{\infty} \frac{-1}{2\pi} \left[\frac{\cos n\theta_y}{r_y^n} r^{n-1} \sin n\theta - \frac{\sin n\theta_y}{r_y^n} r^{n-1} \cos n\theta \right] \sin\theta \\ &\quad + a_2 \sum_{n=1}^{\infty} \frac{-1}{2\pi} \left[\frac{\cos n\theta_y}{r_y^n} r^{n-1} \cos n\theta + \frac{\sin n\theta_y}{r_y^n} r^{n-1} \sin n\theta \right] \sin\theta \\ &\quad + a_2 \sum_{n=1}^{\infty} \frac{-1}{2\pi} \left[-\frac{\cos n\theta_y}{r_y^n} r^{n-1} \sin n\theta + \frac{\sin n\theta_y}{r_y^n} r^{n-1} \cos n\theta \right] \cos\theta. \end{aligned}$$

Then, we have

$$\begin{aligned} -\frac{\partial F}{\partial r}\Big|_{r=r_e} &= a_1 \sum_{n=1}^{\infty} \frac{n-1}{2\pi} \left[\frac{\cos n\theta}{r_y^n} r_e^{n-2} \cos n\theta + \frac{\sin n\theta}{r_y^n} r_e^{n-2} \sin n\theta \right] \cos\theta \\ &\quad + a_1 \sum_{n=1}^{\infty} \frac{n-1}{2\pi} \left[\frac{\cos n\theta}{r_y^n} r_e^{n-2} \sin n\theta - \frac{\sin n\theta}{r_y^n} r_e^{n-2} \cos n\theta \right] \sin\theta \\ &\quad + a_2 \sum_{n=1}^{\infty} \frac{n-1}{2\pi} \left[\frac{\cos n\theta}{r_y^n} r_e^{n-2} \cos n\theta + \frac{\sin n\theta}{r_y^n} r_e^{n-2} \sin n\theta \right] \sin\theta \\ &\quad + a_2 \sum_{n=1}^{\infty} \frac{n-1}{2\pi} \left[-\frac{\cos n\theta}{r_y^n} r_e^{n-2} \sin n\theta + \frac{\sin n\theta}{r_y^n} r_e^{n-2} \cos n\theta \right] \cos\theta \end{aligned}$$

Therefore we have

$$
\begin{aligned}
& -\frac{\partial F}{\partial r}\Big|_{r=r_e} \\
= \;& a_1 \sum_{n=1}^{\infty} \frac{n-1}{2\pi} r_e^{n-2} \left[\frac{\cos n\theta_y}{r_y^n} \cos(n-1)\theta + \frac{\sin n\theta_y}{r_y^n} \sin(n-1)\theta \right] \\
& + a_2 \sum_{n=1}^{\infty} \frac{n-1}{2\pi} r_e^{n-2} \left[-\frac{\cos n\theta_y}{r_y^n} \sin(n-1)\theta + \frac{\sin n\theta_y}{r_y^n} \cos(n-1)\theta \right] \\
= \;& a_1 \sum_{n=1}^{\infty} \frac{n}{2\pi} r_e^{n-1} \left[\frac{\cos(n+1)\theta_y}{r_y^n} \cos n\theta + \frac{\sin(n+1)\theta_y}{r_y^n} \sin n\theta \right] \\
& + a_2 \sum_{n=1}^{\infty} \frac{n}{2\pi} r_e^{n-1} \left[-\frac{\cos(n+1)\theta_y}{r_y^n} \sin n\theta + \frac{\sin(n+1)\theta_y}{r_y^n} \cos n\theta \right].
\end{aligned}
$$

Thus we have

$$
g_e^n + g_e^{-n} = \frac{n}{2\pi} r_e^{n-1} \Big(\frac{a_1 \cos(n+1)\theta_y + a_2 \sin(n+1)\theta_y}{r_y^{n+1}} \Big), \tag{7}
$$

$$
i(g_e^n - g_e^{-n}) = \frac{n}{2\pi} r_e^{n-1} \Big(\frac{a_1 \sin(n+1)\theta_y - a_2 \cos(n+1)\theta_y}{r_y^{n+1}} \Big) \tag{8}
$$

for $n \geq 1$. From (7) and (8), we have

$$
\begin{aligned}
g_e^n = \frac{n}{4\pi} r_e^{n-1} \Big(& \frac{a_1 \cos(n+1)\theta_y + a_2 \sin(n+1)\theta_y}{r_y^{n+1}} \\
& - i \frac{a_1 \sin(n+1)\theta_y - a_2 \cos(n+1)\theta_y}{r_y^{n+1}} \Big),
\end{aligned} \tag{9}
$$

$$
\begin{aligned}
g_e^{-n} = \frac{n}{4\pi} r_e^{n-1} \Big(& \frac{a_1 \cos(n+1)\theta_y + a_2 \sin(n+1)\theta_y}{r_y^{n+1}} \\
& + i \frac{a_1 \sin(n+1)\theta_y - a_2 \cos(n+1)\theta_y}{r_y^{n+1}} \Big)
\end{aligned} \tag{10}
$$

for $n \geq 1$.

3. The pointwise behavior of the potential in the shell

In this section we compute numerically the solution V_δ given by (5) using (9) and (10). Observe that there are three parameters for the dipole source $f(x) = a \cdot \nabla \delta_y(x)$, that is, the direction a, the radius (distance from origin and the source) r_y, and the angle θ_y. We vary them to see how the solution varies accordingly. We fix the annulus $\Gamma_i = \{(x, y) \in \mathbb{R}^2 | x^2 + y^2 = 1\}$ and $\Gamma_e = \{(x, y) \in \mathbb{R}^2 | x^2 + y^2 = 2^2\}$ throughout this section.

3.1. Varying the dipole directions and angle.

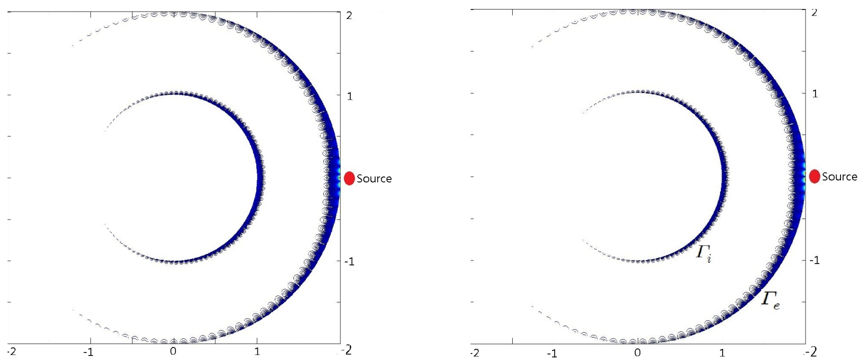

(A) $\left|\frac{\partial V_\delta}{\partial r}\right|$ (B) $\left|\frac{\partial V_\delta}{\partial \theta}\right|$

FIGURE 1. level curves in the shell $r_i = 1, r_e = 2$ and the source $a = (1, 0), r_y = 2.1, \theta_y = 0$.

Figure 1 shows the level curves of the solution when $a = (1, 0), r_y = 2.1, \theta_y = 0$. We draw 1000 numbers level curves in descending order. This means that $\left|\frac{\partial V_\delta}{\partial r}\right|$ and $\left|\frac{\partial V_\delta}{\partial \theta}\right|$ would attain higher values in the dark region. One can easily see that dark region is distributed along the interface Γ_i, Γ_e which is close to the dipole source(red point).

Figure 2 shows graphs of the solution when we change the dipole angle θ_y while fixing the dipole direction $a = (1, 0)$ and $r_y = 2.1$. It seems that $|\frac{\partial V_\delta}{\partial r}|$ has the maximum on the Γ_e and $\theta = \theta_y$. So, we can easily expect that $|\frac{\partial V_\delta}{\partial r}|$ and $|\frac{\partial V_\delta}{\partial \theta}|$ may have the maximum on the Γ_e and $\theta = \theta_y$. Figure 3 shows the height of the $|\frac{\partial V_\delta}{\partial \theta}|$ along the Γ_e when using the same source used in Figure 2 (A).

On the other hand, $|\frac{\partial V_\delta}{\partial \theta}|$ attains its maximum near $\theta = 0$ but not at $\theta = 0$. Figure 4 shows similar phenomenon when we change dipole direction a. One can easily see that $|\frac{\partial V_\delta}{\partial r}|$ and $|\frac{\partial V_\delta}{\partial \theta}|$ attain those maximum near $\theta = \theta_y = 0$ but not at $\theta = 0$.

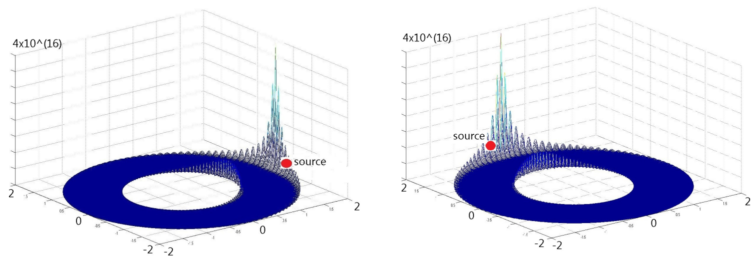

(A) $\theta_y = 0$ (B) $\theta_y = \frac{\pi}{2}$

FIGURE 2. height of the $\left|\frac{\partial V_\delta}{\partial r}\right|$ in the shell $r_i = 1, r_e = 2$ and $r_y = 2.1, a = (1, 0)$.

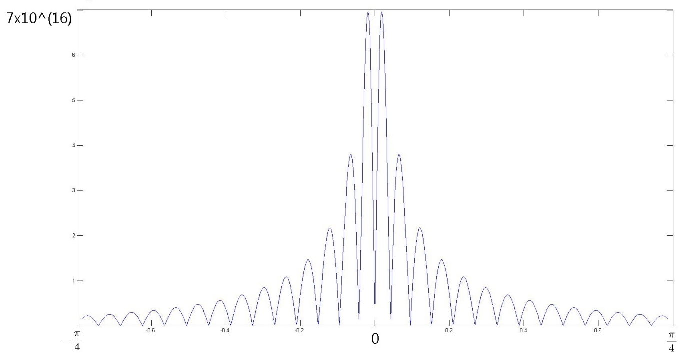

FIGURE 3. $x-$axis is the angle $-\frac{\pi}{4} \leq \theta \leq \frac{\pi}{4}$ and $y-$axis is $\left|\frac{\partial V_\delta}{\partial \theta}\right|$ at the $r = 2$ and the same source used in Figure 2 (A).

3.2. Varying the dipole distance.

The key observation here from numerical simulation is that there is an radius r_0 such that if $r_y \leq r_0$, then

$$\max_{r = r_i} \left|\frac{\partial V_\delta}{\partial r}\right| \leq \max_{r = r_e} \left|\frac{\partial V_\delta}{\partial r}\right|, \tag{11}$$

and if $r_y \geq r_0$, then

$$\max_{r = r_i} \left|\frac{\partial V_\delta}{\partial r}\right| \geq \max_{r = r_e} \left|\frac{\partial V_\delta}{\partial r}\right|. \tag{12}$$

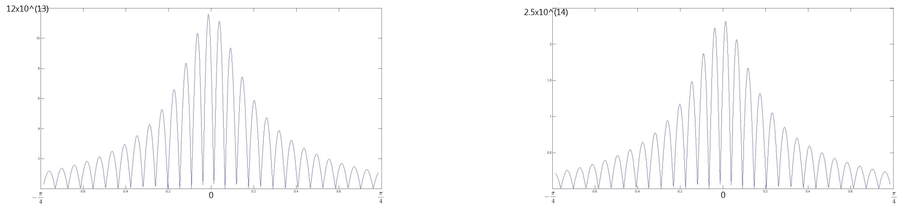

(A) $\left|\frac{\partial V_\delta}{\partial r}\right|$ (B) $\left|\frac{\partial V_\delta}{\partial \theta}\right|$

FIGURE 4. given dipole source is $a = (1, 1), r_y = 2.3, \theta_y = 0$.

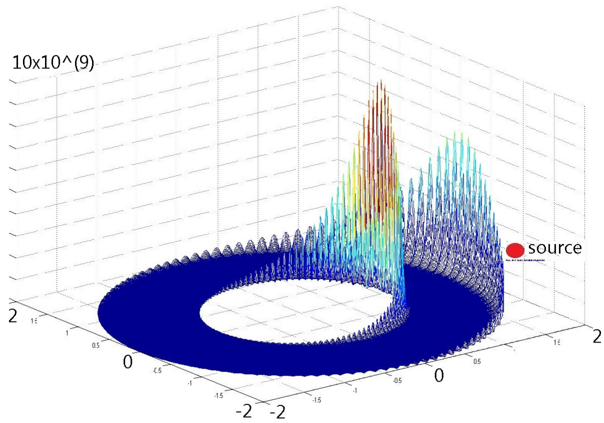

FIGURE 5. $\left|\frac{\partial V_\delta}{\partial r}\right|$ in the shell and $a = (1, 0), r_y = 2.7, \theta_y = 0$.

Figure 2 (A) shows that the maximum of $|\frac{\partial V_\delta}{\partial r}|$ on Γ_e is larger than that on Γ_i if r_y is small. On the other hand Figure 5 shows that (12) holds if r_y is large.

3.3. Comparison of the real and imaginary parts.

Figure 6 (A) and (B) show that only the real part of $\frac{\partial V_\delta}{\partial r}$ and $\frac{\partial V_\delta}{\partial \theta}$ contributes to the resonance on the Γ_i. On the other hand, Figure 6 (C) and (D) show that only the imaginary part of $\frac{\partial V_\delta}{\partial r}$ and $\frac{\partial V_\delta}{\partial \theta}$ contributes to the resonance on the Γ_e.

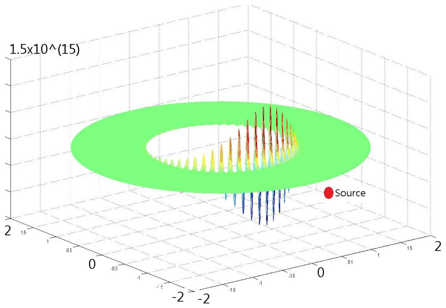

(A) real part of $\frac{\partial V_\delta}{\partial r}$

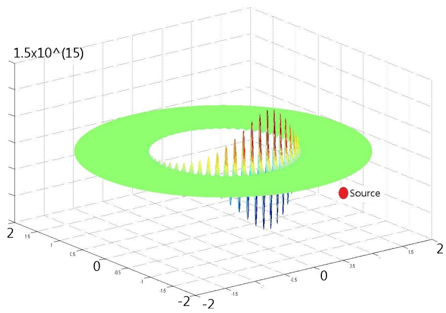

(B) real part of $\frac{\partial V_\delta}{\partial \theta}$

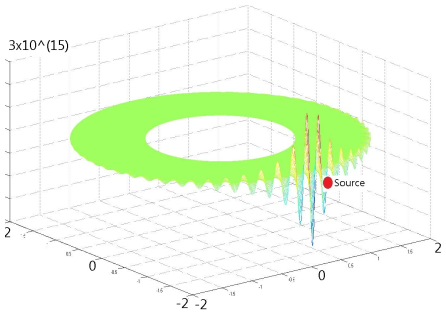

(C) imaginary part of $\frac{\partial V_\delta}{\partial r}$

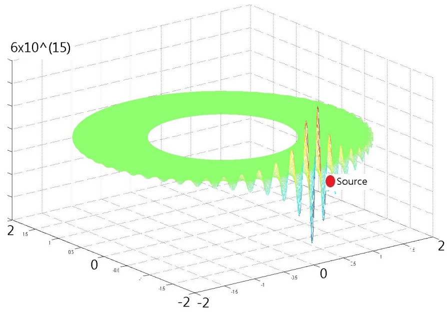

(D) imaginary part of $\frac{\partial V_\delta}{\partial \theta}$

FIGURE 6. given dipole source is $a = (1, 2), r_y = 2.2, \theta_y = \frac{3\pi}{2}$.

4. Conclusions

We investigated point-wise behavior of solutions by numerical simulations. Interesting queations which arise through our investigation include (i) there is $r_0 > 0$ such that if $r_y \leq r_0$, then $\max_{r=r_i} \left|\frac{\partial V_\delta}{\partial r}\right| \leq \max_{r=r_e} \left|\frac{\partial V_\delta}{\partial r}\right|$, and if $r_y \geq r_0$, then $\max_{r=r_i} \left|\frac{\partial V_\delta}{\partial r}\right| \geq \max_{r=r_e} \left|\frac{\partial V_\delta}{\partial r}\right|$ (ii) $\mathrm{Re}(\nabla V_\delta)$ is bounded on Γ_e independently of δ and $\mathrm{Im}(\nabla V_\delta)$ is bounded on Γ_i independently of δ. We will look into these questions in rigorous way in future.

References

[1] H. Ammari, G. Ciraolo, H. Kang, H. Lee and G.W. Milton, *Spectral theory of a Neumann-poincaré-type operator and analysis of cloaking due to anomalous localized resonance*, Arch. Rational Mech. Anal. **208** (2013), 667–692.

[2] H. Ammari, G. Ciraolo, H. Kang, H. Lee and G.W. Milton, *Anomalous localized resonance using a folded geometry in three dimensions*, Proc. R. Soc. A **469** (2013), 20130048.

[3] H. Ammari, G. Ciraolo, H. Kang, H. Lee and G.W. Milton, *Spectral theory of a Neumann-Poincaré-type operator and analysis of anomalous localized resonance II*, Contemporary Math. **615** (2014), 1–14.

[4] O.P. Bruno and S. Lintner, *Superlens-cloaking of small dielectric bodies in the quasi-static regime*, J. Appl. Phys. **102** (2007), 124502.

[5] D. Chung, H. Kang, H. Lee, K. Kim and H. Lee, *Cloaking due to anomalous localized resonance in plasmonic structures of confocal ellipses*, (2014).

[6] R.V. Kohn, J. Lu, B. Schweizer and M.I. Weinstein, *A variational perspective on cloaking by anomalous localized resonance*, Commun Math Phys **328** (2014), 1–27.

[7] G.W. Milton and N.-A.P. Niorovici, *On the cloaking effects associated with anomalous localized resonance*, Proc. R. Soc. A **462** (2006), 3027–3059.

[8] G.W. Milton, N.-A.P. Nicorovici, R.C. McPhedran, *Opaque perfect lenses*, Physica B **394** (2007), 171–175.

[9] G.W Milton, N.-A.P. Nicorovici, R.C. McPhedran and L.C. Botten, *Quasistatic cloaking of two-dimensional polarizable discrete systems by anomalous resonance*, Optics Express **15** (2007), 6314–6323.

Junyong Eom
Department of Mathematics
Inha University
Incheon 402-751, Korea
E-mail: jyeom@inha.edu